IOP Conf. Series: Materials Science and Engineering **452** (2018) 042164 doi:10.1088/1757-899X/452/4/042164

Study on Braking Characteristics of Regenerative Brake-By-Wire System Based on Mechanical-Electron-Magnetism Integration for Electric Vehicles

Zhongfu Zhang[1, a], Changran He[2, *], Jun Xu[1], Guizhen Yu[1] and Guoye Wang[2]

[1]School of Transportation Science and Engineering, Beihang University, Beijing 100191, China
[2]Vehicle and Traffic Engineering Department, China Agricultural University, Beijing 100083, China

*Corresponding author e-mail: 934455433@qq.com, [a]992263218@qq.com

Abstract. For the disadvantages of current electric vehicles regenerative braking, a new design of regenerative brake-by-wire system based on mechanical-electron-magnetism integration is proposed. The new system has electromagnetic braking mode and hybrid braking mode, the former uses electromagnetic braking and the latter combines electromagnetic braking with friction braking. In the hybrid braking mode, the new system can realize friction braking without extra actuator energy. To research the braking characteristics and braking principle of the regenerative brake-by-wire system, the vehicle dynamic model is established. The braking performance and energy recovery efficiency of the system are studied under emergency braking condition. The results show the regenerative brake-by-wire system based on mechanical-electron-magnetism integration not only meets brake comfort under low braking strength and stability under high braking strength, and brake efficiency, but also has better braking response and robustness. With the feature of variable pedal ratio, it conforms to driver's pedal feeling. The control parameters are reduced and the performance of control system is improved. The new braking system can maintain a high recovery efficiency in a wide range of brake strength and increase the driving range of electric vehicles effectively.

1. Introduction

In recent years, the low carbon policy has made hybrid vehicles and fully electric vehicles popular [1]. Electric vehicles is an effective way to solve the problems of energy shortage and pollution, and the regenerative braking of motor has become an important way to save energy [2-4]. The electric vehicles is easy to achieve high recovery efficiency of braking energy [5-6], and regenerative braking provides an effective way of extending the driving range of battery powered electric vehicles [7]. According to statistics, about 50% of the driving energy is consumed by braking system in urban driving condition [8-9]. Therefore, it is of great significance to improve the recovery efficiency of braking energy for reducing energy consumption and increasing the driving range of electric vehicles [10-11].

There are two main types of braking energy recovery technology existing in current electric vehicles, one is composite of hydraulic braking and motor regenerative braking [12-13], and the other is composite of electronic mechanical braking and motor regenerative braking [14-15]. The former can only provide regenerative braking force for the driving wheel [16], the kinetic energy cannot be well captured during braking process. The latter uses the method of Electromechanical Brakes in combination with regenerative braking so braking force can be distributed to front and rear axles according to an optimal curve [17]. Therefore, more regenerative braking force will be distributed to the driven wheel, which will offer more kinetic energy for regenerative braking [15]. But they need a set of independent friction braking system to participate in work at the same time to achieve the braking energy recovery [18]. The current regenerative braking system remains many issues, for example, it has complicated structure, more control parameters, and low recovery efficiency, and it is difficult to control concertedly and guarantee braking performance. Moreover, it consumes actuated energy, etc [18].

To solve the disadvantages of regenerative braking system applied to current electric vehicles, a new design of regenerative brake-by- wire system based on mechanical-electron- magnetism integration (hereinafter referred to as MEM) is proposed. When providing electromagnetic braking and energy feedback, it actuates friction braking and realizes mechanical-electron-magnetism coupled regenerative braking.

2. Construct of MEM System

Combined with the advantages of EMB and regenerative braking, and according to the coupled interaction among machine, electron and magnetism, the MEM is built based on in-wheel motors. The structure of MEM is illustrated in Fig. 1. The new system is mainly composed of two parts, electromagnetic braking system and friction braking system. Electromagnetic braking system includes wheel, transmission, motor rotor and stator, etc. Friction braking system includes splined sleeve, screw, nut, guide-block, thrust bearing, elastic element, brake caliper and brake disc, etc.

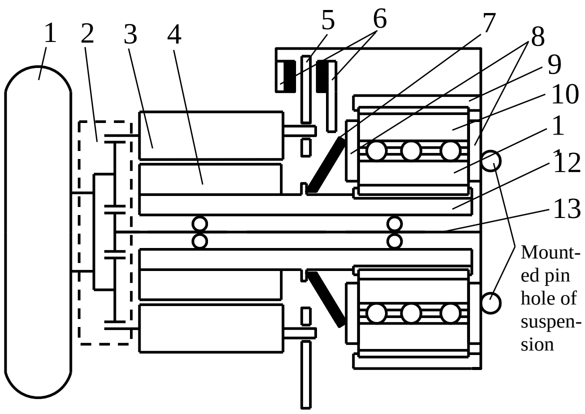

Figure 1. Structure of regenerative brake-by- wire system based on mechanical-electron-magnetism integration

1 wheel, 2 transmission, 3 motor rotor, 4 motor stator, 5 brake disc, 6 brake caliper, 7 elastic element, 8 thrust bearing, 9 guide-block, 10 nut, 11 screw, 12 splined sleeve, 13 fixed device

When braking, the motor is in the state of power and in the control of motor controller to generate electricity for charging the accumulator. The electromagnetic torque between the motor rotor and stator is transferred from the motor rotor to wheel by transmission, which hinders the wheel from rotating and thus braking force is produced between wheel and ground. And the relationship of motor rotor and stator is action and reaction. Therefore, the electromagnetic torque between the motor rotor and stator is transferred from the motor stator to screw by splined sleeve at the same time. The splined sleeve is fixed on motor stator and connected to screw through sliding spline. The splined sleeve is supported by fixed device but it can freely rotate. The screw and nut are joined by non-locking spiral.

The rotation of nut is limited by guide-block, so the nut just slides along the axial direction. Therefore, the screw and nut are driven by splined sleeve and slide along opposite direction. The right thrust bearing limits their axial displacement, so the nut or screw can only push the left thrust bearing to move.

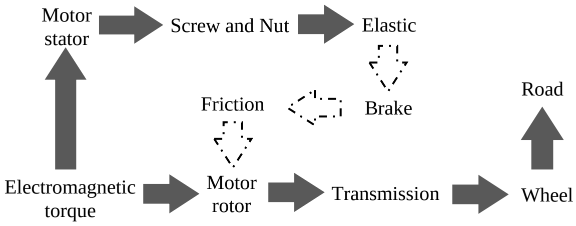

Figure 2. Electromagnetic braking mode

Under low braking strength condition, the push produced by smaller electromagnetic torque is unable to overcome the elastic force of elastic element. Then the space between thrust bearing and brake caliper cannot be eliminated, so the brake disc is not clamped and cannot prompt friction torque to hinder the wheel rotate. The process of electromagnetic braking mode is shown in Fig. 2.

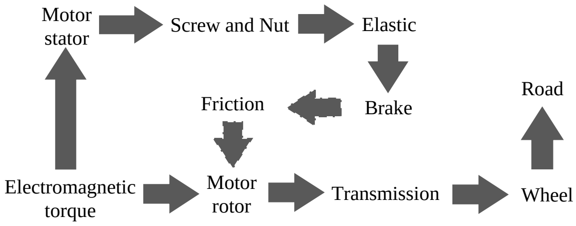

Figure 3. Hybrid braking mode

Under high braking strength condition, the push produced by larger electromagnetic torque is able to overcome the elastic force of elastic element. Then the space between thrust bearing and brake caliper can be eliminated, so thrust bearing push brake caliper to clamp the brake disc and generates friction torque. The friction torque acting on the motor rotor forms coupled braking torque with electromagnetic torque between the motor rotor and stator. And the coupled braking torque hinders the wheel rotate. The process of hybrid braking mode is shown in Fig. 3.

The MEM system is coupled brake-by-wire system that integrates regenerative braking and friction braking. The electromagnetic braking torque produced through electric energy feedback actuates friction braking, so it can realize friction braking without extra actuator energy of friction braking. The electromagnetic braking and friction braking form mechanical-electron-magnetism coupled system and work together to realize vehicle braking.

3. Vehicle Braking Dynamic Model Based on MEM System

The key component of mechanical-electron-magnetism coupled regenerative brake-by-wire system is a screw driving mechanism. As is shown in Fig. 4 and Fig. 1, the screw is driven to rotate by splined sleeve fixed on motor stator. The screw rotates along with splined sleeve and can slide along the splined sleeve. The nut cannot rotate and only can slide along the guide-block. The screw and nut are joined by non-locking spiral.

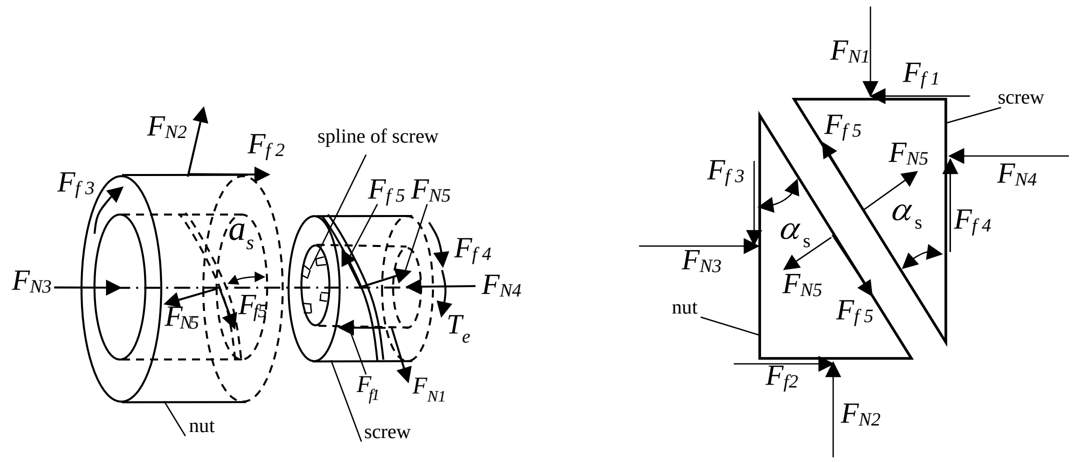

(a) (b)

Figure 4. Dynamic model of MEM

As is shown in Fig. 4, T_e is the electromagnetic torque on motor stator, which acts on the screw through splined sleeve. F_{N1}, F_{N2}, F_{N3}, F_{N4} and F_{N5} are normal force on contact surface of screw spline, normal force on sliding surface of nut, end plane force of nut, end plane force of screw, normal force on spiral surface of screw and nut. F_{f1}, F_{f2}, F_{f3}, F_{f4} and F_{f5} are frictional forces of friction pairs that above-mentioned forces act on. α_s is the lead angle of spiral. The dynamic equation of non-locking spiral transmission is written as:

$$\begin{cases} F_{fi} = f_i F_{Ni} \left(1,2,\cdots,5\right) \\ T_e = F_{N1} \cdot R_{c1} \\ T_e - \left(F_{N5}\sin\alpha_s + F_{f5}\cos\alpha_s\right) \cdot R_{c5} - F_{f4}R_{c4} = J_{Lg}\dot{\omega}_{Lg} \\ F_{N5}\cos\alpha_s - F_{f5}\sin\alpha_s - F_{N4} - F_{f1} = 0 \\ \left(F_{N5}\sin\alpha_s + F_{f5}\cos\alpha_s\right) \cdot R_{c5} - F_{N2} \cdot R_{c2} - F_{f3}R_{c3} = J_{Lm}\dot{\omega}_{Lm} \\ F_{N3} + F_{f2} + F_{f5}\sin\alpha_s - F_{N5}\cos\alpha_s = 0 \\ T_e - F_{N2} \cdot R_{c2} - F_{f4} \cdot R_{c4} - F_{f3} \cdot R_{c3} = J_{Lg}\dot{\omega}_{Lg} + J_{Lm}\dot{\omega}_{Lm} \\ F_{N3} + F_{f2} = F_{N4} + F_{f1} \end{cases} \tag{1}$$

Where f_1, f_2, f_3, f_4 and f_5 are frictional coefficients of above-mentioned friction pairs. R_{c1}, R_{c2}, R_{c3}, R_{c4} and R_{c5} are meshing radius of screw spline, sliding radius of nut, friction radius on end plane of nut, friction radius on end plane of screw, meshing radius on spiral surface of screw and nut. J_{Lg} and J_{Lm} are rotational inertia of screw and nut. ω_{Lg} and ω_{Lm} are angular velocities of screw and nut, other parameters are same as above.

The electromagnetic torque (T_e) acting on motor stator generates end plane force of nut (F_{N3}), end plane force of screw (F_{N4}) through the transmission. And the end plane force of nut or screw acts on the left thrust bearing and generates thrust force (F_N). Then F_N overcomes the elastic force (F_s) of elastic element and acts on the brake disc. Friction torque acts on the motor rotor through pin and then produces friction braking torque (T_{bc}) on wheel through the transmission. As is shown in Fig. 5, wheel is mainly affected by friction braking torque (T_{bc}) and electromagnetic braking torque (T_{be}) from MEM system and braking force (F_x) from ground during vehicle braking.

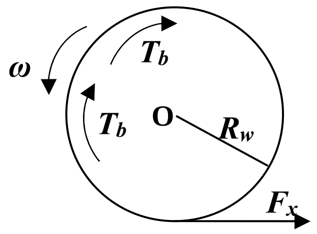

Figure 5. Dynamic model of wheel

The dynamic equation of wheel is written as:

$$\begin{cases} T_{be} = i_c \eta_c \cdot T_e \\ T_{bc} = i_c \eta_c \cdot 2\mu_c \left(F_N - F_s\right) \cdot R_p \, , \\ F_x R_w - T_{bc} - T_{be} = J_w \dot{\omega}_w \end{cases} \tag{2}$$

Where T_{be} is electromagnetic braking torque, T_{bc} is friction braking torque, i_c is transmission ratio from motor rotor to wheel, η_c is efficiency from motor rotor to wheel, F_s is elastic force of elastic element, μ_c is friction coefficient of brake disc, R_p is action radius of brake disc, ω_w is angular velocity of wheel, J_w is rotational inertia of wheel, R_w is rolling radius of wheel, F_x is longitudinal force of tire, other parameters are same as above.

As is shown in Fig. 6, three DOF nonlinear vehicle dynamic equation is written as:

$$\begin{cases} m\dot{v}_x - mv_y\omega_z = \sum F_x \\ m\dot{v}_y + mv_x\omega_z = \sum F_y \\ I_z\dot{\omega}_z = \sum M_z \end{cases} \tag{3}$$

Where m is entire mass of vehicle, I_z is yaw inertia of vehicle, v_x is longitudinal velocity of vehicle, v_y is lateral velocity of vehicle, ω_z is yaw rate of vehicle, $\sum F_x$ is longitudinal resultant, $\sum F_y$ is lateral resultant, $\sum M_z$ is yaw moment acting on barycenter of vehicle, other parameters are same as above.

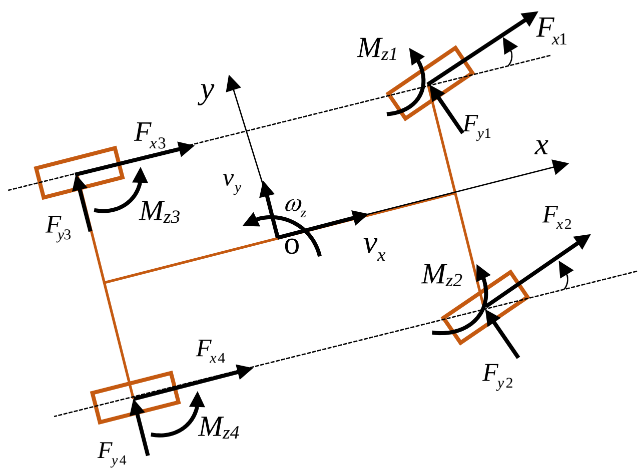

Figure 6. Dynamic model of vehicle

As is shown in Fig. 6, force equation of vehicle is written as:

$$\begin{cases} \sum F_x = F_{x1}\cos\delta_1 - F_{y1}\sin\delta_1 + F_{x2}\cos\delta_2 \\ \qquad - F_{y2}\cdot\sin\delta_2 + F_{x3} + F_{x4} - \dfrac{C_d A_f}{21.15} v_x^2 \\ \sum F_y = F_{x1}\sin\delta_1 + F_{x2}\sin\delta_2 + F_{y1}\cos\delta_1 \\ \qquad + F_{y2}\cos\delta_2 + F_{y3} + F_{y4} \\ \sum M_z = \begin{bmatrix} F_{x1}\sin\delta_1 + F_{x2}\sin\delta_2 + \\ F_{y1}\cos\delta_1 + F_{y2}\cos\delta_2 \end{bmatrix} \cdot l_f \\ \qquad - \begin{bmatrix} F_{x1}\cos\delta_1 - F_{x2}\cos\delta_2 - \\ F_{y1}\sin\delta_1 + F_{y2}\sin\delta_2 \end{bmatrix} \cdot \dfrac{B_f}{2} \\ \qquad - \left(F_{y3} + F_{y4}\right)\cdot l_r - \left(F_{x3} - F_{x4}\right)\cdot \dfrac{B_r}{2} \\ \qquad + M_{z1} + M_{z2} + M_{z3} + M_{z4} \end{cases} \tag{4}$$

Where F_{xi} is longitudinal force of each tire, F_{yi} is lateral force of each tire, M_{zi} is aligning torque of each tire, δ_1 and δ_2 are steering angles of LF wheel and RF wheel, l_f and l_r are distances from barycenter to front axle and from barycenter to rear axle, B_f and B_r are distances of front wheels and rear wheels, other parameters are same as above.

During one braking, the power loss of electric vehicles braking energy mainly consists of copper loss (P_{Cu}) and iron loss (P_{Fe}), inverter loss (P_{inv}) and charge loss (P_{bat}). The recovery efficiency of braking energy is written as [10]:

$$\eta_e = \frac{\int_0^t \left(T_e\omega_e - P_{Cu} - P_{Fe} - P_{inv} - P_{bat}\right) dt}{E_V + E_J} \tag{5}$$

Where η_e is recovery efficiency of braking energy, T_e is electromagnetic torque, ω_e is angular velocity of motor rotor, E_V is vehicle translational energy loss, E_J is vehicle rotational energy loss, other parameters are same as above.

4. Principle Analysis of MEM System

By Eqs. (1) and the former dynamic model of MEM, the thrust force (F_N) can be expressed as a function of the electromagnetic torque (T_e), as shown in Eqs. (6):

$$F_N = g\left(T_e\right) \tag{6}$$

When the thrust force is unable to overcome the elastic force of elastic element, F_N and F_s are action and reaction. F_s reaches a peak point (F_{s0}) and remains stable when the space between thrust bearing and brake caliper is eliminated. Eq. (7) expresses the change process of elastic force (F_s):

$$F_s = \begin{cases} F_N & F_N \le F_{s0} \\ F_{s0} & F_N > F_{s0} \end{cases} \tag{7}$$

By Eqs. (2), (6), (7) and the former dynamic model of wheel, the normal force on brake caliper (F_c) is explained by Eq. (8):

$$F_c = \begin{cases} 0 & F_N \le F_{s0} \\ g\left(T_e\right) - F_{s0} & F_N > F_{s0} \end{cases} \tag{8}$$

So the friction braking torque can be written as Eqs. (9) according to Eqs. (2) and (8):

$$T_{bc} = k_c \left[g\left(T_e\right) - F_s \right] \tag{9}$$

Where k_c is related ratio.

By Eqs. (2) and (9), the total braking torque (T_b) can be expressed as a function of the electromagnetic torque (T_e), as shown in Eqs. (10):

$$T_b = \begin{cases} k_e T_e & F_N \le F_{s0} \\ k_e T_e + k_c \left[g\left(T_e\right) - F_{s0} \right] & F_N > F_{s0} \end{cases} \tag{10}$$

Where k_e is related ratio.

So the total braking torque (T_b) can be written as:

$$T_b = f\left(T_e\right) \tag{11}$$

The total braking torque (T_b) is a function for one-to-one correspondence about single variable (T_e). Therefore, the control variable of regenerative braking system is reduced and the performance of control system is improved.

With the aim of conforming to driver's pedal feeling, the pedal ratio is variable. The electromagnetic torque is written as:

$$T_e = \begin{cases} k_1 T_{pedal} & T_{pedal} \le PEDAL \\ k_2 T_{pedal}^2 + k_3 T_{pedal} + k_4 & T_{pedal} > PEDAL \end{cases}, \tag{12}$$

Where T_{pedal} is pedal travel, $PEDAl$ is the control point of pedal travel, k_1, k_2, k_3 and k_4 are related coefficients.

According to the former dynamic model of MEM system, the simulation model of new-type regenerative braking system is established based on Matlab/Simulink. The experimental parameters are shown in Table 1.

Table 1. Experimental parameters

Parameter	Value
lead angle of spiral /(deg)	5
friction coefficient of brake disc	0.35
action radius of brake disc /(m)	0.13
transmission ratio(i_c)	3
peak point of elastic force /(N)	25000
peak torque of motor /(N.m)	120

The braking principle of MEM system is studied by simulation. The braking force and torque with electromagnetic torque are analyzed, and the braking force and torque with pedal travel are analyzed.

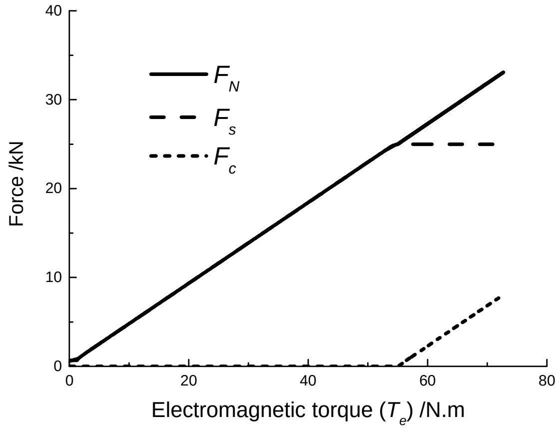

Figure 7. Force and electromagnetic torque

As is shown in Fig. 7, it explains the relationship between force and electromagnetic torque. The trust force (F_N) is unable to overcome the elastic force of elastic element (F_s) when T_e varies within a certain range. So F_N is equal to F_s and the normal force on brake caliper (F_c) remains at 0. Therefore, the total braking torque (T_b) is equal to electromagnetic braking torque (T_{be}) and friction braking torque (T_{bc}) remains 0, as shown in Fig. 8. After a certain electromagnetic torque, the friction braking starts to work and the elastic force (F_s) approaches the maximum and remains at the peak. And F_N keeps increasing with T_e. So F_c begins to increase linearly with T_e. Therefore, T_b and T_{bc} increase rapidly with T_e, as shown in Fig. 8.

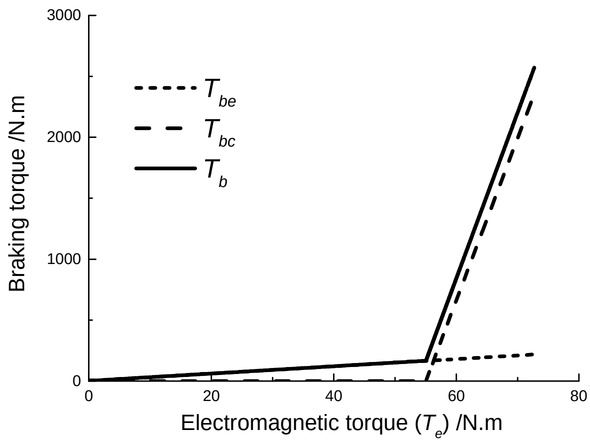

Figure 8. Braking torque and electromagnetic torque

Fig. 8 shows the relationship between the total braking torque (T_b), electromagnetic braking torque (T_{be}), friction braking torque (T_{bc}) and electromagnetic torque (T_e).

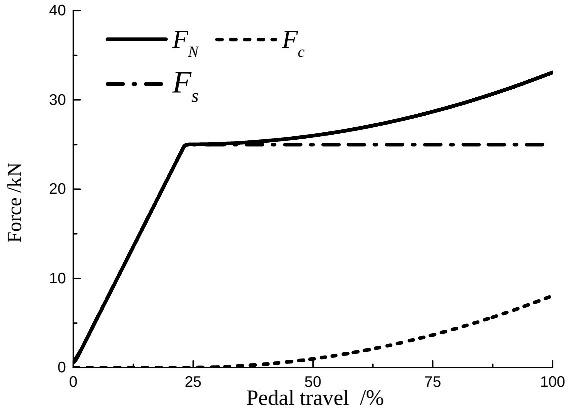

Figure 9. Force and pedal travel

Fig. 9 explains the relationship between trust force (F_N), elastic force (F_s), normal force (F_c) and pedal travel.

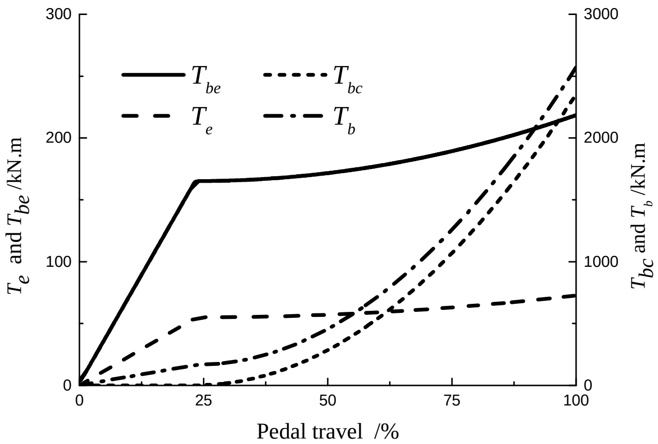

Figure 10. Torque and pedal travel

As is shown in Fig. 10, it explains the relationship between torque and pedal travel. The trust force (F_N) produced by smaller electromagnetic torque (T_e) is unable to overcome the elastic force (F_s). When $T_{pedal} \leq PEDAL$, as shown in Fig. 9. Then F_N is equal to F_s and F_c remains at 0. Therefore, T_b is equal to T_{be} and T_{bc} remains at 0, as shown in Fig. 10. After a certain pedal travel ($PEDAL$), the space between thrust bearing and brake caliper is eliminated and F_s approaches the maximum and stays the same. Then F_N keeps increasing with pedal travel and F_c begins to increase rapidly with pedal travel. Likewise, T_b and T_{bc} increase rapidly with pedal travel, as shown in Fig. 10.

5. Properties Analysis of MEM System

According to the former dynamic models of vehicle and MEM system, the complete vehicle simulation model of new-type braking system is established based on CarSim and Matlab/Simulink. The small passenger car used for simulation has four wheels of electromagnetic-mechanical coupled regenerative braking system, and experimental parameters are shown in Table 2. The braking performance of MEM system is studied under emergency braking condition. And the brake comfort, brake efficiency, follow performance of pedal and recovery efficiency of braking energy are analyzed and verified by simulation.

Table 2. Experimental parameters

Parameter	Value
car mass/(kg)	1300
rolling radius of wheel /(m)	0.3
peak power of motor /(kW)	11
rated speed of motor /(r/min)	1500
initial speed of braking /(km/h)	60
road friction coefficient	0.85
braking force distribution coefficient	0.526

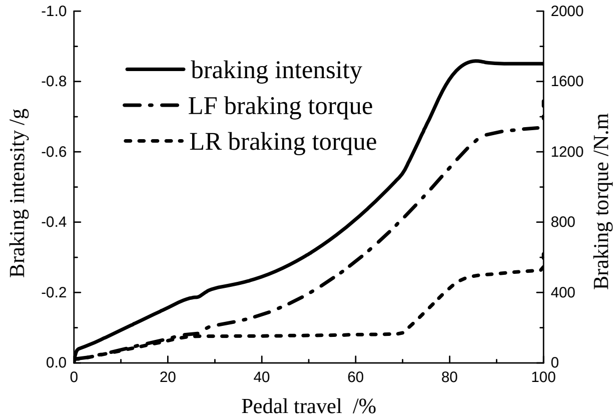

Figure 11. Braking strength and pedal travel

As is shown in Fig. 11, it can acquire fast braking response when initial braking. Braking strength and pedal travel have a good linear relationship under low braking strength condition. Friction braking is effective and braking strength increases exponentially with the pedal travel under high braking strength condition. And it can meet the need of high braking strength under emergency braking. The braking torque of front and rear wheels can well satisfy the matching relation between the front wheel's braking force distribution coefficient and the rears'. So it satisfies the braking requirements and purposes of driver during driving process. The relationship of braking strength and pedal travel is consistent with the braking tests. Comparing with conventional hydraulic braking system, the new braking system (MEM) holds better compositive performances such as brake efficiency under high braking strength, brake comfort under low braking strength, follow performance of pedal, braking force distribution and brake response.

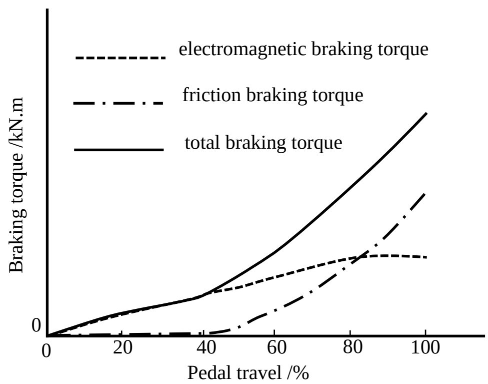

Figure 12. Braking torque and pedal travel

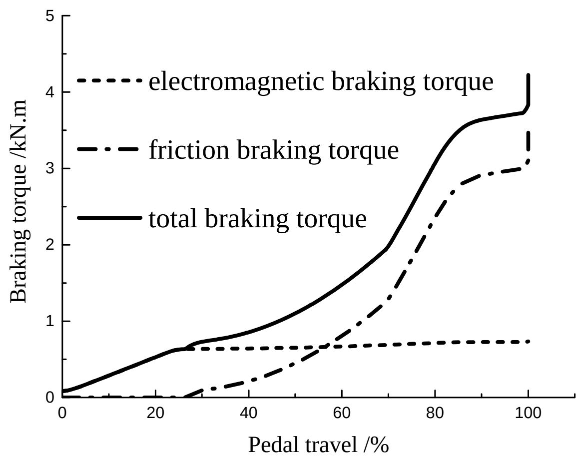

Figure 13. Braking torque and pedal travel

The performance curve of present electrical-hydraulic regenerative braking system is shown in Fig. 12. In order to improve recovery efficiency, the air travel of hydraulic brake pedal should be long as much as possible on the premise of meeting brake efficiency and ensuring brake comfort. The performance curve of MEM is shown in Fig. 13. Similarly, the friction braking doesn't work under low braking strength. After a certain pedal travel, electromagnetic braking torque approaches the maximum. Then friction braking torque and total braking force increase linearly with the pedal travel. When pedal travel is close to the maximum, friction braking torque and total braking torque increase rapidly on high braking strength condition. Compared with the present electric-hydraulic regenerative braking system, electromagnetic braking torque of MEM is closer to the maximum under medium braking strength. Under general road condition, medium braking strength is most frequently used during driving process, so the new braking system (MEM) can enhance recovery efficiency of braking energy obviously. In addition, MEM doesn't need a set of independent hydraulic braking system. And it only needs a set of by-wire system, so the new braking system simplifies the structure of brake system.

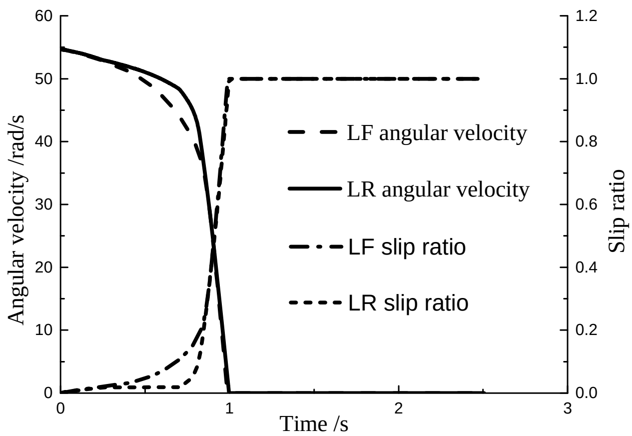

Figure 14. Angular velocity and slip ratio

As is shown in Fig. 14, the changes of front and rear wheels speed are smooth and consistent. The wheel is locked when slip ratio climbs to 1.0 smoothly. Angular velocity of front wheels descends and slip ratio of front wheels increases rapidly, so front wheels are more easily locked than rear wheels through braking force distribution on emergency braking. It meets the requirement of brake stability. Hence the new braking system (MEM) has a good brake comfort and brake stability.

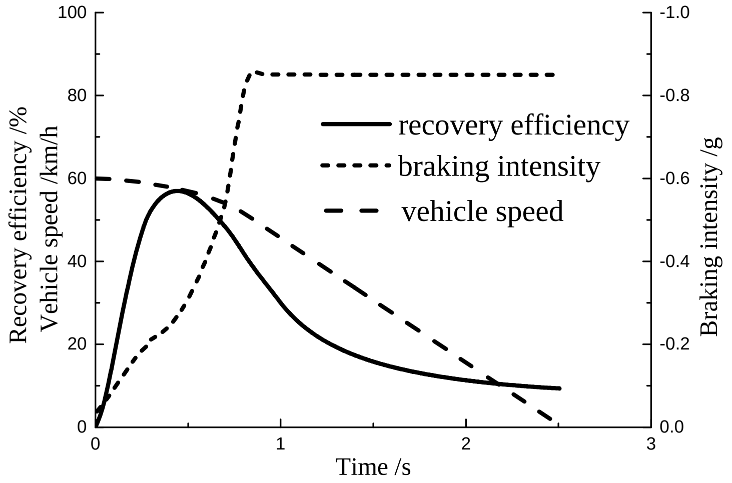

Figure 15. Recovery efficiency of braking energy

As is shown in Fig. 15, with the increase of braking strength the vehicle speed goes down smoothly and recovery efficiency of brake energy increases firstly and then decreases. After braking strength approaches the maximum, the vehicle speed slows down linearly and recovery efficiency decreases slowly. The recovery efficiency reaches its maximum of 56.9% when braking strength is 0.27g and vehicle speed is 57.5 km/h, and recovery efficiency still approaches 50% when braking strength is 0.49g and vehicle speed is 54.6 km/h. It has higher recovery efficiency of brake energy under frequently used low-medium braking strength of 0.2 ~ 0.4g and urban driving cycle with low-medium vehicle speed of 50 km/h, and it has recovery efficiency of 9.3% under emergency braking. Therefore, the new braking system (MEM) improves total recovery efficiency of brake energy during one driving greatly and increases the driving range of electric vehicles effectively.

6. Conclusion

(1) MEM system not only meets brake comfort under low braking strength and brake stability under high braking strength, but also has better braking force distribution and brake response.

(2) With the feature of variable pedal ratio, MEM system conforms to driver's pedal feeling.

(3) In the premise of assuring the braking performance, MEM system adopts integrated by-wire system and simplifies the structure of brake system without a set of independent hydraulic braking system. The control variable is reduced and the performance of control system is improved.

(4) MEM system has higher recovery efficiency of brake energy under low-medium braking strength and low-medium vehicle speed conditions, and it remains a definite recovery efficiency under emergency braking. Therefore the new braking system improves total recovery efficiency of brake energy greatly and increases the driving range of electric vehicles effectively.

Acknowledgments

This work was financially supported by National Natural Science Foundation of China (Grant No. 51175498) fund.

References

[1] González-Gil A, Palacin R, Batty P, et al. A systems approach to reduce urban rail energy consumption [J]. *Energy Conversion and Management*, 2014, 80: 509-524.
[2] Clarke P, Muneer T, Cullinane K. Cutting vehicle emissions with regenerative braking [J]. *Transportation Research Part D: Transport and Environment*, 2010, 15 (3): 160-167.
[3] Zhang R, Yao EJ. Eco-driving at signalised intersections for electric vehicles [J]. *IET Intelligent Transport Systems*, 2015, 9 (5): 488-497.

[4] Zhao Y, Deng WW, Wu J., et al. Torque control allocation based on constrained optimization with regenerative braking for electric vehicles [J]. *International journal of automotive technology*, 2017, 18 (4): 685-698.
[5] Gao Y, Chen L, Ehsani M. Investigation of the Effectiveness of Regenerative Braking for EV and HEV [R]. *SAE Technical Paper*, 1999.
[6] González-Gil A, Palacin R, Batty P. Sustainable urban rail systems: Strategies and technologies for optimal management of regenerative braking energy [J]. *Energy Conversion and Management*, 2013, 75: 374-388.
[7] Long B, Lim S T, Ryu J H, et al. Energy-regenerative braking control of electric vehicles using three-phase brushless direct-current motors [J]. *Energies*, 2013, 7 (1): 99-114.
[8] Walker A M, Lamperth M U, Wilkins S. On friction braking demand with regenerative braking [R]. *SAE Technical Paper*, 2002.
[9] González-Gil A, Palacin R, Batty P, et al. A systems approach to reduce urban rail energy consumption [J]. *Energy Conversion and Management*, 2014, 80: 509-524.
[10] LU Dongbin, OUYANG Minggao, GU Jing, et al. Optimal regenerative braking control for permanent magnet synchronous motors in electric vehicles [J]. *Proceedings of the Chinese Society for Electrical Engineering*, 2013, 33 (3): 83-91. (in Chinese)
[11] Li Z, Chowdhury M, Bhavsar P, et al. Optimizing the performance of vehicle-to-grid (V2G) enabled battery electric vehicles through a smart charge scheduling model [J]. *International Journal of Automotive Technology*, 2015, 16 (5): 827-837.
[12] Dinçmen E, Güvenç B A. A control strategy for parallel hybrid electric vehicles based on extremum seeking [J]. *Vehicle* System *Dynamics*, 2012, 50 (2): 199-227.
[13] Zou Z, Cao J, Cao B, et al. Evaluation strategy of regenerative braking energy for supercapacitor vehicle [J]. *ISA Transactions*, 2015, 55: 234-240.
[14] D Jianlong Z, Chengliang Y I N, Jianwu Z. Design and Analysis of Electro-mechanical Hybrid Anti-lock Braking System for Hybrid Electric Vehicle Utilizing Motor Regenerative Braking [J]. *Chinese Journal of Mechanical Engineering*, 2009, 22 (1): 42-49.
[15] Zhou ZG, Mi C, Zhang GX. Integrated control of electromechanical braking and regenerative braking in plug-in hybrid electric vehicles [J]. *International Journal of Vehicle Design*, 2012, 58 (2-4): 223-239.
[16] Zhao Guozhu, Teng Jianhui, Wei Minxiang, et al. Study on low-speed regenerative braking of electric vehicle as ABS based on fuzzy control [J]. *Journal of Mechanical Engineering*, 2012, 23 (1): 117-121.
[17] Ahn J K, Jung K H, Kim D H, et al. Analysis of a regenerative braking system for hybrid electric vehicles using an electro-mechanical brake [J]. *International Journal of Automotive Technology*, 2009, 10 (2): 229-234.
[18] Ko J W, Ko S Y, Kim I S, et al. Co-operative control for regenerative braking and friction braking to increase energy recovery without wheel lock [J]. *International journal of automotive technology*, 2014, 15 (2): 253-262.